

# ORIGINAL RESEARCH ARTICLE

## PERFORMANCE EVALUATION OF THERMALLY AND ACID-ACTIVATED SMECTITE IN BLEACHING PALM OIL

---

### ABSTRACT

Smectite from Ubulu-uku was activated thermally and chemically to increase its adsorptive performance. The thermally and chemically modified samples were analyzed using X-ray Fluorescence (XRF). Thermal activation involved drying in the sun for 24 hours, milling it to a particle size of 0.212 mm and heating at a temperature range of 150 to 750 °C (150, 300, 450, 600, and 750 °C). The chemical activation was carried out by immersing the samples in 100 mL of a hydrochloric acid solution. It was determined what the physicochemical properties were, including acidity, cation exchange capacity, oil retention, and surface area. The samples' adsorptive abilities were then evaluated by bleaching palm oil using them. The X-ray fluorescence results showed that the chemical compositions of the samples were altered by both thermal and acid treatments. There were some disappearances of the stretching bands at 3692, 3525, and 1104  $\text{cm}^{-1}$  assigned to the H-O-H stretching. The surface area was also observed to increase in value with the thermal treatment until the temperature reached 600 °C. The physicochemical results indicated that the chemically activated samples have a larger surface area, acidity, and lower cation exchange capacity with a bleaching efficiency of 95.8%. In comparison, the thermally activated samples have a lower surface area, acidity, and high cation exchange capacity with a bleaching efficiency of 89.7%. This study has revealed that the performance of local clay minerals can be enhanced by thermal and acid activation.

*Keywords:* [Acid Activation, Physicochemical Properties, Bleaching, Thermal Treatment, Smectite]

### 1. INTRODUCTION

The morphological, mineralogical, chemical, and thermal characteristics of clay minerals, such as smectite, vary, and their exchange behavior is also different [1]. Clay minerals are naturally used in many industrial applications, such as the food, chemical, and paper industries, due to their great variability [2,3]. Nevertheless, using the clay minerals unmodified (chemical and thermal treatments) isn't always feasible. By changing the clay's structure, modification can increase its surface area and adsorption capacities [4].

Acid processing of clay minerals, specifically fiber-rich clays [5,6,7,8], smectites [9,10,11,12] and Kaolinite, which is frequently used to improve their physicochemical behavior in an effort to achieve better industrial properties [13]. After treating sepiolite with acid, [14] came to the conclusion that the resulting silica could be competitive with precipitation-derived silica in a variety of industrial applications. Because acid treatment increases the specific surface area and number of active sites of the solids, it is commonly referred to as acid activation of clay minerals.

By disaggregating particles, possibly removing mineral impurities, and removing metal-exchange cations, this treatment changes the surfaces of clays. According to [15], acid-treated clay minerals are commonly used for the commercial purposes of bleaching or decolorizing oils. They are also applied in the fields of adsorption and catalysis [16,17].

Clay materials are heated to high temperatures in order to thermally treat the minerals in clay [18]. The type of clay, particle size, and heating range all have a significant impact on how the heated clays change in structure and chemical composition [19]. To get rid of any contaminants and moisture that may have adhered to the clay particle, the clay minerals are burned [1]. Initially, weight loss and an increase in surface area are caused by the removal of the hydrated and adsorbed water and impurities attached to the clay particles during the dehydration stage. This opens up additional adsorption sites [19]. Additional heating results in the de-hydroxylation. The surface functional groups and the structure of the clay are changed if the heating is prolonged past the point of dehydroxylation. The links inside the clay structure break, causing the structure to collapse and its surface area to decrease [19,20].

Although extensive research has been conducted on acid and thermal activation of clay minerals, there is limited focus on their application in bleaching palm oil using locally sourced smectite from Ubulu-

uku. Numerous studies demonstrated that heat and acid treatments of certain clay minerals enhance their catalytic and adsorbent properties; strong treatments, on the other hand, may introduce an opposite behavior, reducing this activity [21,22,23,24]. Smectite is a lamellar-shaped hydrated aluminum silicate, making it easily pliable to water and other polar molecules. Because of this, smectites have extremely strong plastic and colloidal characteristics. Their physical characteristics also vary depending on the type of exchangeable cations that neutralize the structure and their composition, which can shift in octahedral locations.

In this work, smectite from Ubulu-uku was altered by thermal and acid treatment to enhance its capacity for absorption. The modified samples were analyzed and characterized to investigate the impacts of the different modification methods. To examine the samples' adsorptive abilities, palm oil was bleached using them.

## **2. MATERIALS AND METHODS**

### **2.1 Materials**

Clay substance with a grey hue from Ubulu-uku (N: 6° 16' 00"; E: 6° 55' 00"; A: 118m) in Delta state, Nigeria was employed as the main raw material. An oil mill located at Isuofia (N: 6° 1' 60"; E: 7° 2' 60"; A: 361m), in Aguata, Anambra state, Nigeria produced the refined palm oil used. Analytical grade chemicals bought from Conraws Company Ltd, Enugu, were all that were used.

### **2.2 Experimental Methods**

#### **2.2.1 The clay sample's thermal activation**

Thermal activation was used to alter the physical properties of the clay material. After 24 hours of drying in the sun, the mined clay was cleaned and milled to a particle size of 0.212 mm. A crucible containing 20 g of the sized sample was measured and put in a muffle furnace. During a predetermined 90-minute period, the thermal activation was carried out throughout a temperature range of 150 to 750 °C (150, 300, 450, 600, and 750 °C). Following the activation period, the samples were removed and allowed to cool for four hours in a desiccator. The numbered labels on the samples—UB0, UB150, UB300, UB450, UB600, and UB750—indicate the calcination temperatures that were employed in the investigation.

#### **2.2.2 The clay sample's acid activation**

The clay material was ground to a particle size of 0.212 mm and allowed to air dry before being activated. A 250 mL flask was filled with 10 g of the prepared sample and 100 mL of a hydrochloric acid solution. The resultant suspension was heated for two hours and thirty minutes to 90 °C on a hot plate that was magnetically agitated. The resultant slurry was put into a Buchner funnel at the conclusion of the experiment in order to separate the clay and acid. Using a pH tester, the remaining clay was repeatedly cleaned with distilled water until the neutral point was reached. For four hours, the clay residue was dried in an oven set to 80 °C. After being dried, the samples were crushed and re-screened to a particle size of 0.212 mm. An additional round of activation was conducted using varying acid concentrations (1.5–6.5 mol L<sup>-1</sup>) of HCl. The resulting clay samples were given the following labels: UB0, UB1.5, UB2.5, UB3.5, UB4.5, UB5.5, and UB6.5. The numbers on the labels represent the quantities of acid that were employed in the activation process.

### **2.3 Evaluation of the clay samples' characteristics**

The samples of natural, acid-treated, and thermally-activated clay were analyzed to identify their chemical and mineralogical constituents. Using samples generated using the traditional KBr disc method, the chemical composition was ascertained using an X-ray fluorescence (XRF) Philips PW 2400 XRF spectrometer, and the mineralogical composition was ascertained using a Fourier transform infrared (FTIR) Shimadzu S8400 spectrophotometer.

#### **2.3.1 Specific surface area**

[25,26] description of ethylene glycol mono-ethyl-ether (EGME) was used to calculate the surface area. Samples of clay were ground through a No. 40 sieve after being sun-dried. After removing the water, a tiny portion of the sample was dried with P<sub>2</sub>O<sub>5</sub> and kept in an oven overnight at 105 °C. The dried sample

was weighted ( $W_a$ ) with an analytical balance that had a 0.001 g accuracy level after one gram was distributed out into the bottom of the aluminum tare. Using a pipette, around 3.0 mL of laboratory-grade EGME was added to the sample, and it was gently swirled to generate a homogenous slurry. To quantify the surface area precisely, the EGME was used to every clay sample. After that, the aluminum tare was put inside a typical laboratory vacuum desiccator that was sealed with glass and given 20 minutes to acclimate. The vacuum pump was then used to remove the desiccator. After 12, 16, and 24 hours, the aluminum tare was taken out of the desiccator and weighed ( $W_s$ ). The sample was put back in the desiccator and evacuated for two more hours if its mass changed by more than 0.001 g between two measurements. Until the sample mass did not change by more than 0.001 g, the procedure was repeated. The following is how the surface area was expressed:

$$A = \frac{W_a}{0.000286W_s} \quad (1)$$

where  $A$  = surface area ( $\text{m}^2 \text{g}^{-1}$ ),  $W_a$  = weight of EGME retained by the sample and  $W_s$  = weight of  $\text{P}_2\text{O}_5$ -dried sample. According to [27], 0.000286 is the weight of EGME needed to build a uni-molecular layer on a surface area of one square meter.

### **2.3.2 Cation Exchange Capacity (CEC) [28]**

Using a magnetic stirrer, 5 g of the clay sample were weighed and placed into a 250 mL polythene bottle. Weighing both the bottle and its contents ( $M_1$ ). After adding 100 milliliters of buffered barium chloride solution to the bottle, it was shaken for a full hour on a magnetic stirring plate. The bottle was centrifuged at 1500 rpm for 15 minutes at the conclusion of the period, and the supernatant was disposed of. After adding 200 mL more of the buffered barium chloride solution, the mixture was stirred for an additional hour on a magnetic stirring plate. Overnight, the bottle and its contents were left. The bottle and its contents were centrifuged at 1500 rpm for 15 minutes the next day, and the supernatant was disposed of. On the magnetic stirring plate, 200 mL of distilled water was introduced and stirred for a few minutes. The supernatant was disposed of after it was centrifuged for an additional fifteen minutes. Weighing both the bottle and its contents ( $M_2$ ). After thoroughly mixing 100 milliliters of  $\text{MgSO}_4$  solution using a pipette, the mixture was placed on the magnetic stirring plate and allowed to stand for two hours, stirring now and then. Two hours later, the contents were centrifuged for fifteen minutes at 1500 rpm, and the supernatant was poured into a stoppered bottle. Pipette 5 mL of this solution into a 100 mL conical beaker, followed by the addition of 5 mL of ammonia buffer and 6 drops of indicator. Titer A1 milliliters of standard EDTA were used to titrate this mixture. Five milliliters of an aliquot of 0.05 M  $\text{MgSO}_4$  solution (titer B mL) were used for another titration. A shift in color from blue to pink denoted the endpoint. This is how the Cation Exchange Capacity was determined:

$$CEC = 8 \left\{ B - \frac{(A_1 \times (100 + M_2 - M_1))}{100} \right\} \left( \frac{meq}{100g} \right) \quad (2)$$

Where  $CEC$  = cation-exchange capacity ( $\text{meq} (100\text{g})^{-1}$ ),  $M_1$  = weight of bottle plus dry content (g),  $M_2$  = weight of bottle plus wet content (g),  $A_1$  = titration end-point of the sample (mL), and  $B$  = titration end-point of  $\text{MgSO}_4$  solution (mL)

### **2.3.3 Measurement of acidity**

100 mL of distilled water were mixed with 10 g of clay. The concoction was given a good shake. Next, a pH meter was used to determine the pH of the clay suspension. 10 g of clay was put to a 3-minute boil in 10 mL of distilled water for the acidity test. After that, it was filtered and given another 100 mL of distilled water wash. After that, 0.1 N NaOH solutions were used to titrate the filtrate and wash liquid together to the phenolphthalein endpoint. Afterwards, the percentage weight of NaOH per gram of clay was used to determine the acidity:

$$\text{Acidity} = \left[ \frac{V \times N \times 40}{W_c} \right] \times 100 \quad (3)$$

where  $W$  is the weight of clay (g),  $N$  is the amount of sodium hydroxide, and  $V$  is the volume of sodium hydroxide used in the titration (mL).

### **2.3.4 Oil retention (OR) [29,30]**

After mixing 100 g of oil and 10 g of clay, the mixture was heated to 120 °C for five minutes and then

maintained there for an additional five minutes. A suction apparatus was used to filter the mixture for thirty minutes. After filtering, the cake was weighed. The percentage oil retention was calculated as:

$$\%OR = \frac{W_c [(100 - \%H_2O \text{ in cake}) - 10(100 - \%H_2O \text{ in clay})]}{10} \quad (4)$$

Where OR represents oil retention,  $W_c$  is the weight of the cake (g). The percent of  $H_2O$  in cake and clay was determined by drying them in an oven at  $110^\circ C$  until the weight change was negligible.

## 2.4 Bleaching experiment

Batch processing was used to carry out the bleaching trials. Two grams of activated clay samples were added to a 250-milliliter beaker along with 50 grams of refined palm oil. The clay and oil mixture were heated to  $80^\circ C$  for 30 minutes while being constantly stirred in a water bath. The resulting slurry was filtered using dry filter paper after the reaction was complete. The color of the bleached oils was then measured using a UV-Vis spectrophotometer (Shimadzu UV mini 1240) set to 450 nm in order to ascertain the bleaching capacity of the acid-activated clays. The bleaching efficiency of the acid-activated clay was calculated in this study using the following equation [31]:

$$\% \text{ Bleaching efficiency} = \frac{(A_{\text{unbleached}} - A_{\text{bleached}})}{A_{\text{unbleached}}} \quad (5)$$

Where  $A_{\text{unbleached}}$  and  $A_{\text{bleached}}$  are the absorbencies of the unbleached and bleached oils, respectively.

## 3. RESULTS AND DISCUSSIONS

### 3.1 Result of the clay samples' characteristics

#### 3.1.1 Fourier Transform Infrared (FTIR) spectroscopy analysis

Figures 1 and 2 display the spectra of the untreated and 5.5 mol L<sup>-1</sup> HCl-treated samples, respectively. To investigate the impact of acid-leaching on the clay mineral, FTIR spectra of the raw and acid-leached clay samples were acquired in the 400–4000 cm<sup>-1</sup> range. The changes in the functional groups indicate the modifications that occurred during the activation process [32,33]. During the acid-leaching of the clay samples, the protons from the acid medium penetrated the clay structures attacking the OH groups thereby causing the alteration in the adsorption bands attributed to the OH vibrations and octahedral cations. The intensities of the stretching bands observed at 3449, 1639, and 792 cm<sup>-1</sup> (associated with O-H, along with Al-OH stretch) decreased after acid activation. The increase in the severity of acid caused the disappearance of the stretching bands at 3692, 3525, and 1104 cm<sup>-1</sup> assigned to the H-O-H stretching. After acid leaching, the peak designated to the Si-O-Si stretch at 472, 685, 920, 1037, 1037, and 3626 cm<sup>-1</sup> survived, albeit with a modest rise in intensity; other researchers found similar results [2,34]. Following the acid treatment, the tetrahedral transformation happened at 720 cm<sup>-1</sup>, which increased.

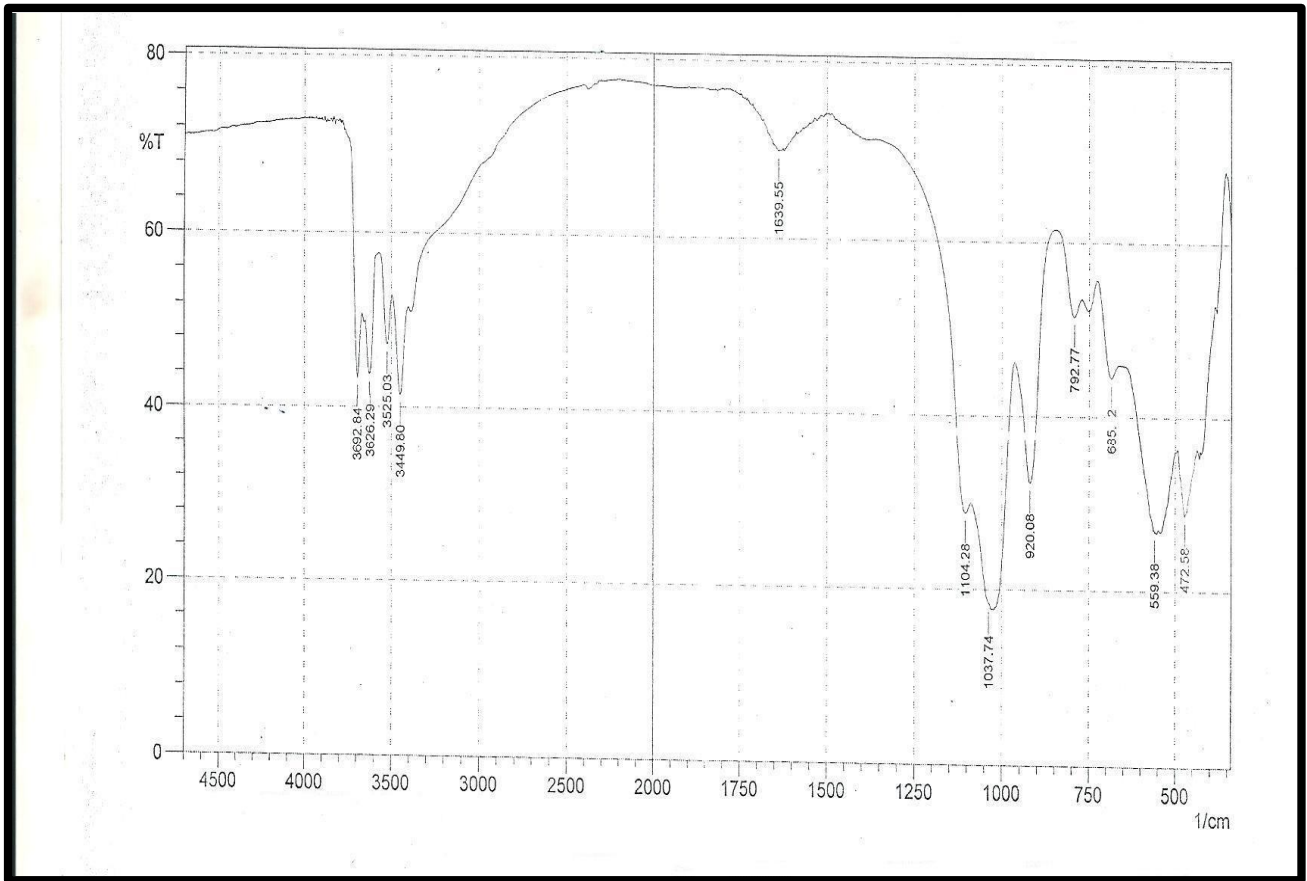
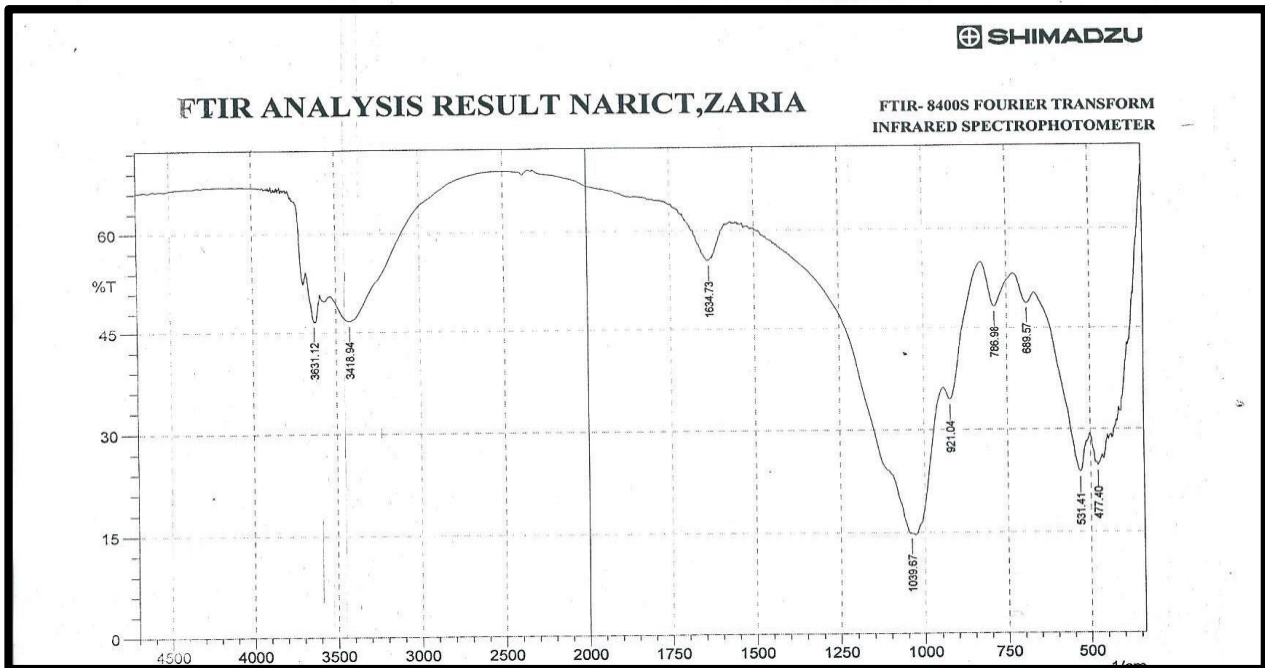


Fig.1.FTIR spectrum of untreated Ubulu-ukuclays sample.



### **3.1.2 Result of the clay sample's thermal activation**

Table 1 presents the findings from the chemical analysis of the thermally activated Ubulu-uku clay samples. The primary chemical compositions, according to the data, are oxides of Si, Fe, and Al, together with various mineral oxides of K, Na, Mg, Ca, and other elements. When the calcined samples were compared to the raw sample, it was seen that the oxides rose up to 600 °C throughout the calcination process and then stayed constant at higher temperatures. This may be explained by the clay structure's total loss of organic materials and water. It was observed that the CEC of the thermally activated samples reduced as the temperature rose (Table 1). This decline in CEC was ascribed by [35] to the deformation associated with the CaM layers. Due to reversible dehydration, CEC significantly reduces when the temperature rises to 600 °C. Irreversible dehydration and de-hydroxylation cause the space between the 2:1 CaM layers to gradually contract as the temperature rises beyond 600 °C, which also gradually reduces swelling. The reason for the quick fall in CEC is the increasing difficulty of the barium chloride cations in aqueous solution to penetrate the CaM interlayer. Considering that the interlayer has largely crumbled.

The results of the variance in surface area with thermal activation are presented in Table 1. From the table, it can be observed that the surface area showed an increase in value until the thermal treatment reached 600 °C, and at higher temperatures, there was an abrupt fall in the value. [36] suggested that this parallel variation showed that the surface area stems from the walls of the micro and meso pores. [37] stated that the reduction in surface area during thermal activation may be due to the loss of raw material caused by the effect of increased temperatures. As the temperature increases from 600 °C the crystal framework of the minerals found in the clay, like montmorillonite and illite in the bentonite rapidly collapses. Parallel to this collapse as the empty spaces between the layers have been destroyed the pore volume and consequently the surface area drops rapidly. In the original clay mineral, the surface area which is  $98.8\text{m}^2\text{g}^{-1}$  increased by more than 100% and reached its maximum which is  $225.3\text{m}^2\text{g}^{-1}$  as a result of the thermal treatment applied during 2 hr at 600 °C.

Figure 3 displays the findings from the adsorption experiments conducted on the thermally activated samples in bleaching palm oil. The figure illustrates how the adsorption effectiveness rose up to 600 °C and then decreased as the calcination temperature climbed. This may be explained by the fact that samples that were activated beyond 600 °C displayed reduced Si/[Al<sup>3+</sup> + Fe<sup>3+</sup> + Mg<sup>2+</sup>] ratios and surface areas. Similar results were reported by others [38]. This is consistent with the data in Table I, which shows that the thermally activated sample at 600 °C had the largest surface area and hence absorbed more pigments than the other samples. In their 2008 study, [39] examined the adsorption of lead on thermally activated clays and found that as the temperature increased during calcination, physisorbed water was removed, which led to an increase in adsorption. However, as the temperature went further, adsorption reduced due to a decrease in surface area.

### **3.1.3 Result of the clay sample's acid activation**

The results of the X-ray Fluorescence analysis of the acid-activated samples are shown in Table 2. As can be observed from the table, the octahedral cations such as Al<sup>3+</sup>, Fe<sup>3+</sup>, and Mg<sup>2+</sup>, reduced appreciably as the intensity of the acid treatment increased, while the tetrahedral cation, like Si<sup>4+</sup>, increased with the severity of acid treatment. The behavior showed by the Al<sub>2</sub>O<sub>3</sub>, Fe<sub>2</sub>O<sub>3</sub>, and MgO content with progressive acid treatment is related to the progressive dissolution of the clay minerals. The octahedral sheet destruction passes the cations into the solution, while the silica generated by the tetrahedral sheet remains in the solids, due to its insolubility. [23] suggested that this free silica generated by the initial destruction of the tetrahedral sheet is polymerized by the effect of such high acid concentrations and is deposited on the undestroyed silicate fractions, protecting it from further attack. Apart from leaching out of the octahedral and tetrahedral cations, the acid-activated samples showed a decrease in the cation exchange capacity and an increase in the surface area with an increase in the severity of acid treatment as shown in Table 2, but this was observed to reverse for higher acid concentration. The increase in the surface area from the natural to acid-activated samples could be related to the elimination of the exchangeable cations, de-lamination of smectite, and the generation of micro-porosity during the process. The decrease observed for higher acid concentration could be explained by the passivation of the clay from further acid attack by the insoluble silica [23].

Figure 4 displays the bleaching capabilities of the Ubulu-uku smectite samples that were treated with acid. As can be observed in the figure, the acid concentration employed in the activation step grew, so did the bleaching efficiency. This is a result of the removal of the octahedral cations from the smectite structure which creates more active sites for the adsorption of color pigments onto the clay surface. [40] found that the more

the removal of octahedral cations from the bentonite original structure, the better the decolourizing power of the acid-activated sample. The decolourizing power of the acid-activated samples was observed to reach an optimum value at 5.5 mol L<sup>-1</sup> treatment, but as the concentration continued to rise, a decline in that ability was evident. This could be related to the destruction of the clay crystalline structure by the excess acid attack [3]. [41,31,42] reported that increase in bleaching temperature and adsorption time improved the bleaching efficiency by reducing the free fatty acids in the oil.

The cation exchange capacity (CEC) data given in Table 2 showed that there is a sharp decrease in the CEC of 22.3% from sample UB0 to UB2.5. Smectite sample UB4.5 maintained only 54.5% of the initial CEC, while sample UB5.5 possessed only 48.2% of the initial CEC. This progressive decrease in CEC values upon treatment with hydrochloric acid can be understood in terms of the depopulation of octahedral sheets. It is well established that leaching of the octahedral cations (Mg<sup>2+</sup>, Fe<sup>2+</sup>, Al<sup>3+</sup>) results in a reduction of the negative layer charge and therefore of the CEC [43]. The net reduction in CaO content indicated that the Ca<sup>2+</sup> exchange cations were replaced by hydrogen ions and/or polyvalent cations leached from the octahedral sheet. The decrease in the octahedral sheet oxides (Al<sub>2</sub>O<sub>3</sub>, MgO, and Fe<sub>2</sub>O<sub>3</sub>) along with the concomitant increase in silica content proved that the original structure was altered [44].

The acidity of the activated smectite samples was affected by the acid activation process. The acidity of the smectite samples is presented in Table 2. The acidity was observed to increase with an increase in the severity of the acid treatment. It has been observed that the number of acid centers significantly increases in acid-activated clay samples compared with natural samples [45]. [46] reported that Bronsted acid sites are generated by the exchange of inter-lamellar cations with protons and Lewis acid sites correspond to Mg<sup>2+</sup> and Al<sup>3+</sup> present at the edges of octahedral sheets. The Bronsted acidity stems from terminal hydroxyl groups and from bridging oxygen [47]. An enhancement in the acidity of the host matrix following acid treatment has been observed [48] and explained as the number of the matrix protons (on the clay sheets), not associated with the interlayer cations, which may be increased by acid treatment [44].

The activated smectites' acidity had an impact on how well they bleached as well. Sample UB5.5 exhibited the maximum acidity (0.06), which is in excellent agreement with its high bleaching efficiency (94.2%). It was not surprising that the clay mineral's acidity is essential to its bleaching ability. The acidity found in clay minerals is caused by H<sup>+</sup> ions either taking up exchange sites on the surface or by the water hydrating the exchangeable metal cations dissociating [44]:



It may be assumed that the increase in the Bronsted acidity of the clay after acid activation is what initially caused the improvement in bleaching efficiency. Following the process, the surface hydroxyl groups on the fractured alumina sheets in acid-activated clay minerals can form a type of adsorption site:



The protonated AlOH<sub>2</sub><sup>+</sup> structure can function as a strong binding site, allowing pigments and other coloring agents found in palm oil to adhere to it. Similar to how color is removed from oil, surface activity is necessary to remove contaminants such as metals, soaps, and phospholipids [49]. Drawing from the aforementioned results, it is plausible to say that the polar pigments are drawn to the extremely hydrophilic protonated clay framework. On the other hand, the clay material becomes essentially hydrophobic silica by substantial leaching of cations from the octahedral sheet, which is used to adsorb the non-polar coloring materials present in the oil [44].

**Table 1. The chemical composition, surface area, and Si/ [Al + Fe + Mg] ratios of thermally activated and raw Ubulu-uku clay determined by XRF**

Chemical composition	Clay samples					
	UB0	UB150	UB300	UB450	UB600	UB750
Al <sub>2</sub> O <sub>3</sub>	27.21	27.94	28.31	28.60	28.75	28.69
SiO <sub>2</sub>	50.92	54.57	56.55	57.97	59.26	58.29
Fe <sub>2</sub> O <sub>3</sub>	9.36	9.58	9.72	9.94	10.22	10.19

CaO	0.41	0.51	0.51	0.51	0.51	0.51
MgO	3.10	3.35	3.42	3.67	3.83	3.78
K <sub>2</sub> O	0.35	0.49	0.52	0.55	0.59	0.57
TiO <sub>2</sub>	1.24	1.49	1.52	1.57	1.64	1.61
Na <sub>2</sub> O	0.04	0.05	0.05	0.05	0.05	0.05
Surfacearea(m <sup>2</sup> /g)	98.8	125.4	169.8	202.3	225.6	195.8
Si/(Al+Fe+Mg)	1.28	1.34	1.36	1.37	1.38	1.37
Cationexchangecapacity(meg (100g) <sup>-1</sup> )	112	104	98	87	82	80

**Table 2. The chemical composition, surface area, cation exchange capacity, and Si/ [Al + Fe + Mg] ratios of acid activated and raw Ubulu-uku clay determined by XRF**

Chemicalcomposition	Claysamples						
	UB0	UB1.5	UB2.5	UB3.5	UB4.5	UB5.5	UB6.5
Al <sub>2</sub> O <sub>3</sub>	27.21	22.63	16.45	11.54	7.72	3.83	4.76
SiO <sub>2</sub>	50.92	59.31	64.75	69.54	72.51	75.63	75.87
Fe <sub>2</sub> O <sub>3</sub>	9.36	6.72	4.84	3.11	2.23	1.07	1.43
CaO	0.41	0.29	0.21	0.17	0.16	0.15	0.15
MgO	3.10	2.04	1.65	1.03	0.82	0.43	0.49
K <sub>2</sub> O	0.35	0.19	0.08	0.05	0.03	0.03	0.03
TiO <sub>2</sub>	1.24	1.14	1.02	0.98	0.74	0.67	0.59
Na <sub>2</sub> O	0.04	0.02	0.02	0.02	0.01	0.01	0.01
Surfacearea(m <sup>2</sup> g <sup>-1</sup> )	98.77	156.7	194.6	235.8	255.3	297.4	267.5
Si/(Al+Fe+Mg)	1.28	1.89	2.82	4.43	6.73	14.19	11.36
Oilretention	36	39	41	42	44	45	46
Acidity	0.001	0.01	0.03	0.04	0.04	0.06	0.06
Cationexchangecapacity (meg(100g) <sup>-1</sup> )	112	104	87	72	61	54	58

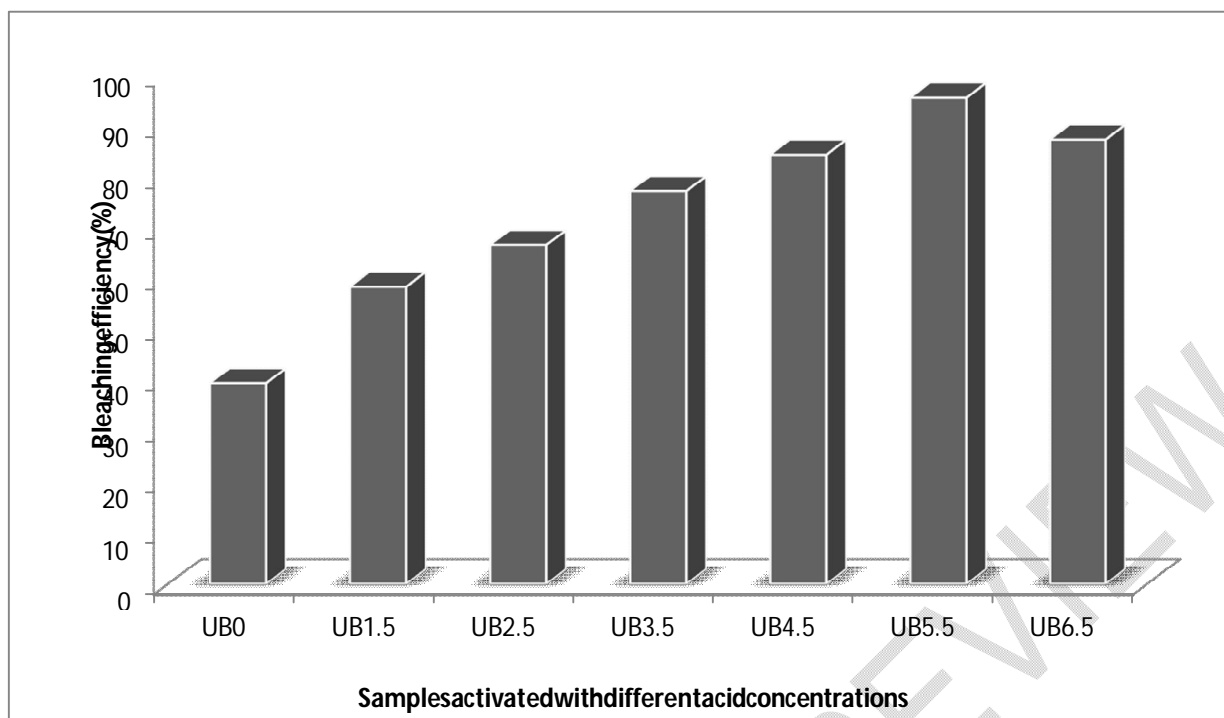


Fig.3. Variation of the bleaching efficiency with calcination temperature

achingEfficiency(%)

**Fig.4. Plot of the bleaching efficiency of the samples activated with different acid concentrations**

#### 4. CONCLUSION

Modification of the Ubulu-uku smectite structure by acid and thermal activation was successfully carried out. The results of both activation methods showed that the clay structure is affected. Attack on the smectite structure after acid treatment is based on the amount of acid present and that of thermal treatment depends on the temperature. The results of these procedures on the characteristics of smectite were examined. by x-ray fluorescence, chemical analysis, and infrared spectrophotometric examination. The activated samples showed high adsorption capacity in bleaching palm oil compared to the untreated sample. The natural smectite's mineralogical composition affected the properties exhibited by the activated samples and these properties enhanced their adsorption capacity.

#### Disclaimer (Artificial intelligence)

Author(s) hereby declare that NO generative AI technologies such as Large Language Models (ChatGPT, COPILOT, etc) and text-to-image generators have been used during writing or editing of manuscripts.

#### REFERENCES

1. Steudel A, Batenburg L, Fischer H, Weidler P, Emmerich K. Alteration of swelling clay minerals by acid activation, *Appl. Clay Sci.* 2009;44:105–115.
2. Christidis, GE, Scott PW, Dunham AC. Acid activation and bleaching capacity of bentonites from the islands of Milos and Chios, Aegean and Greece. *Appl. Clay Sci.* 1997;12:329–347.
3. Diaz F, de Souza SR. Studies on the acid activation of Brazilian smectite clays, *Quim Nova.* 2021;24:343–353.
4. Dai JC, Huang JT. Surface modification of clays and clay-rubber composite. *Appl. Clay Sci.* 1991;15:51–65.
5. Suarez M, Flores Gonzalez L, Rodriguez V, Martin Pozas J. Acid activation of a palygorskite with HCl: Development of physicochemical, textural and surface properties. *Appl. Clay Sci.* 1995;10:247–258.
6. Vicente-Rodriguez M, Lopez-Gonzalez J, Banares-Munoz M. Acid activation of a Spanish sepiolite: Physicochemical characterization, free silica content and surface area of the solids obtained. *Clay Miner.* 1994a;29:361–367.
7. Vicente-Rodriguez MA, Lopez-Gonzalez JD, Banares-Munoz MA. Influence of the free silica generated during acid activation of a sepiolite on the adsorbent and textural properties of the resulting solids. *J. Mater. Chem.*, 1995a;5:127–132.
8. Myriam M, Suarez M, Martin PJ. Structural and textural modifications of palygorskite and sepiolite under acid treatment, *Clays Clay Miner.* 1998;46:225–231.
9. Vicente-Rodriguez M, Suarez-Barrios M, Lopez-Gonzalez J, Banares-Munoz M. Acid activation of a ferrous saponite (griffithite): Physicochemical characterization and surface area of the products obtained. *Clays Clay Miner.* 1994b;42:724–730.
10. Vicente-Rodriguez M, Lopez-Gonzalez J, Banares-Munoz M, Casado-Linarejos J. Acid activation of a Spanish sepiolite II: Kinetics considerations, development of porosity and acid centers and silica fibers size. *Clay Miner.* 1995b;30:315–323.
11. Prieto O, Vicente M, Banares-Munoz M. Acid treatment of a high surface area saponite from Vicalvaro (Madrid,

- Spain). *J. Porous Mater.* 1999;6,345–354.
12. Suarez M, de Santiago C, Garcia Romero E, Pozas J. Textural and structural modifications of saponite from Cerro del Aguila by acid treatment. *Clay Miner.* 2001;36:483 – 488.
  13. Belder C, Banares-Munoz M, Vicente M. Chemical activation of kaolin under acid and alkaline conditions. *Chem. Mater.* 2002;14,234–241.
  14. Xianzhen Y, Chuyi Z. Purification of sepiolite and preparation of silica. *Pro. 9<sup>th</sup> Int. Clay Conf. Strasbourg, 1989. Sci. Geol. Mem.* 1990;89:25–32.
  15. Srasra E, Bergaya F, Vandamme H, Aigub N. Surface properties of an activated bentonite: De-colouration of rape seed oils, *Appl. Clay Sci.* 1988;4:411–421.
  16. Fahn R, Fendler K. Reaction products of organic dye molecules with acid treated montmorillonite. *Clay Miner.* 1983;18:447–458.
  17. Mokaya R, Jones W. Pillared clays and pillared acid-activated clays: A comparative study of physical, acidic and catalytic properties. *J. Porous Mater.* 1995;6,335–344.
  18. Al-Asheh S, Banat F, Abu-Aitah L. Adsorption of phenol using different types of activated bentonites. *Sep. Purification. Technol.* 2003;33:1–10.
  19. Beragaya F, Thang BK, Lagaly G. Modified clays and clay minerals. *Handbook of Clay Science, Development in Clay Science, Vol. 1, Elsevier, The Netherlands; 2009.*
  20. Vimonses V, Lei S, Jin B, Chow C, Saint C. (2009). Kinetic study and equilibrium isotherm analysis of congo red adsorption by clay materials. *Chem. Eng. J.* 2009;148:354–364.
  21. Bonilla JL, Lopez-Gonzalez JD, Ramirez-Saenz A, Rodriguez-Reinoso F, Valenzuela Calahorra C. Activation of a sepiolite with dilute solutions of HNO<sub>3</sub> and subsequent heat treatments: Determination of surface acid centers. *Clay Miner.* 1981;16,173–179.
  22. Gonzalez L, Ibarra L, Rodriguez A, Moya J, Valle F. Fibrous silica gel obtained from sepiolite by hydrochloric acid attack. *Clay Min.* 1989;19:93–98.
  23. Pesquera C, Gonzalez F, Benito L, Blanco C, Mendioroz S, Pajares J. Passivation of a montmorillonite by the silica created in acid activation. *J. Mater. Chem.* 1992;2:907–911.
  24. Dias MI, Suarez MB, Prates S, Martin-Pozas JM. Characterization and acid activation of Portuguese special clays. *Clay Miner.* 1998;38:537–549.
  25. Carter DL, Heilman MD, Gonzalez CL. Ethylene Glycol Mono-ethyl Ether for determining surface area of silicate minerals. *Soil Sci.* 1965;100:356–360.
  26. Carter DL, Mortland MM, Kemper WD. Specific surface. *Methods of soil analysis, Chapter 16, Agronomy, No. 9, Part 1, 2<sup>nd</sup> Ed. American Society of Agronomy.* 1964;456–478.
  27. Chiou CT, Rutherford DW, Manes M. Sorption of N<sub>2</sub> and EGME vapours on some soils, clays, and mineral oxides and determination of sample surface areas by use of sorption data. *Environ. Sci. Technol.* 1993;27:1587–1594.
  28. Inglethorpe SDJ, Morgan DJ, Highley DE, Bloodworth AJ. *Industrial mineral laboratory manual- Bentonite, British Geological Survey Technical Report, WG/93/20; 1990.*
  29. Alexander WT. Process of extruding and treating clay for improved filtration. *European Pat. Appl.* 1988;276-542.
  30. Al-Zahrani AA, Al-Shahrani SS, Al-Tawil YA. Study on the activation of Saudi natural bentonite, Part II: Characterization of the produced active clay and its test as adsorbing agent. *J. King Saudi Uni.* 2000;13(2):193–203.
  31. Nweke CN, Ajemba RO. Clay characterization and bleaching of crude palm oil using acid-activated Nibo clay. *BSTR.* 2022;10(1):14-21. <https://doi.org/10.54987/bstr.v10i1.683>
  32. Nweke CN, Onu CE, Iheanacho CO. Kinetic and thermodynamic studies of crude palm oil bleaching using Amansea clay. *Asian Journal of Applied Chemistry Research.* 2023;13(1):23-42. <https://DOI:10.9734/AJACR/2023/v13i1234>.
  33. Ajemba RO, Nweke CN, Okoye CC, Nwachukwu JO. Adsorption of carotene from crude palm oil by activated Achalla clay. *Journal of Engineering Research and Reports.* 2023;24(5): 1-17. <https://DOI:10.9734/JERR/2023/v24i5813>.
  34. Komandel P, Schmidt D, Medejova J, Cical J. Alteration of smectites by treatment with hydrochloric acid and sodium carbonate solutions, *Appl. Clay Sci.* 1990;5:113–122.
  35. Sarikaya Y, Onal M, Baran B, Alemdaroglu T. The effect of thermal treatment on some of the physicochemical properties of a bentonite. *Clays Clay Min.* 2000;48:557–562.
  36. Onal M, Sarikaya Y, Alemdaroglu T, Bozdogan I. Modification of the adsorptive properties of a bentonite clay. *Commun. Fac. Sci. Univ. Ank. Series B.* 1998;44:15–23.
  37. Lan X, Jiang X, Song Y, Jing X, Xiangdong Xing X. The effect of activation temperature on structure and properties of blue coke-based activated carbon by CO<sub>2</sub> activation. *Green Process Synth.* 2019;8: 837–845. <https://doi.org/10.1515/gps-2019-0054>.
  38. Gonzalez-Pradas E, Villafranca-Sanchez M, Socias-Viciano M, Gallego-Campo A, Urena-Amate D, Fernandez-Perez M. Adsorption of chlorophyll-a from acetone solution on natural and activated bentonite. *J. Chem. Technol. Bio-technol.* 1994;61:175–178.

39. Chaari I, Fakhfakh E, Chakroun S, Bouzid J, Boujelben N, Feki M, Rocha F, Jamoussi F. Lead removal from aqueous solution by Tunisian smectite clay. *J. Hazard. Mater.* 2008;156:545–551.
40. Foletto EL, Volzone C, Porto LM. Performance of an Argentine acid-activated bentonite in the bleaching of soy bean oil. *Braz. J. Chem. Eng.* 2003;20:139–145.
41. Ojewumi ME, Ehinmowo AB, Obanla OR, Durodola BM, Ezeocha, RC. Comparative analysis on the bleaching of crude palm oil using activated groundnut hull, snail shell and rice husk. *Heliyon.* 2021;7(2021)e07747. doi.org/10.1016/j.heliyon.2021.e07747.
42. Nweke CN, Nwokedi IC, Chinyelu CE. Bleaching of crude palm oil by activated Nise clay: Process kinetics, isotherm and thermodynamic Studies. *International Journal of Innovations in Engineering Research and Technology (IJIERT).* 2024;11(2): 55-71.
43. Breen C, Madejova J, Komadel P. Characterization of moderately acid-activated, size-fractionated montmorillonite using IR and MAS NMR spectroscopy and thermal analysis. *J. Mat. Chem.* 1995;5:469–474.
44. Falaras P, Kovanis I, Lezou F, Seiragakis G. Cottonseed oil bleaching by acid-activated montmorillonite. *Clay Miner.* 1999;34:221–232.
45. Vicente Rodriguez MA, Suarez M, Lopez Gonzalez JD, Banares Munoz MA. Characterization, surface area and porosity analyses of the solids obtained by acid leaching of a saponite. *Langmuir.* 1996;12:566–572.
46. Kumar P, Jasra RV, Bhat TSG. Evaluation of porosity and surface acidity in montmorillonite clay on acid activation. *Ind. Eng. Chem. Res.* 1995;34:1440–1448.
47. Laszlo P. Chemical reactions on clays. *Science.* 1987;235:1473–1477.
48. Mokaya R, Jones W. Pillared acid-activated particles. *J. Chem. Soc. Chem. Commun.* 1994;929–930.
49. Morgan DA, Shaw DB, Sidebottom MJ, Soon TC, Taylor RS. The function of bleaching earth in the processing of palm, palm kernel and coconut oils. *J. Am. Oil Chem. Soc.* 1985;62:292–299.